ADVANCED ENGINEERING MATERIALS
www.aem-journal.com

Mass Transfer Performance of Porous Nickel Manufactured by Lost Carbonate Sintering Process

Pengcheng Zhu and Yuyuan Zhao*

Open cell porous metals are excellent electrode materials due to their unique electrochemical properties. However, very little research has been conducted to date on the mass transport of porous metals manufactured by the space holder methods, which have distinctive porous structures. This paper measures the mass transfer coefficient of porous nickel manufactured by the Lost Carbonate Sintering process. For porous nickel samples with a porosity of 0.55–0.75 and a pore size of 250–1500 μm measured at an electrolyte flow velocity of 1–12 cm s^{-1}, the mass transfer coefficient is in the range of 0.0007–0.014 cm s^{-1}, which is up to seven times higher than that of a solid nickel plate electrode. The mass transfer coefficient increases with pore size but decreases with porosity. The porous nickel has Sherwood numbers considerably higher than the other nickel electrodes reported in the literature, due to its high real surface area and its tortuous porous structure, which promotes turbulent flow.

1. Introduction

Porous metals have attracted considerable attention in academia and industry due to their unique combinations of material and structural characteristics, including high surface area, good catalytic ability, high permeability, light weight, good mechanical properties, and so on.[1–9] Open-cell porous metals have been regarded as excellent electrode materials in energy generation and storage.[9–12]

Mass transfer in porous electrodes, that is, the movement of a chemical species from bulk solution to the surface of porous matrix,[13] is critical for the electrochemical reaction, because it is normally the rate-determining step.[14] According to Fick's law, the rate of mass transfer is proportional to the difference between the concentrations in the bulk solution and at the electrode surface and the interfacial area, with the proportionality coefficient being referred to as mass transfer coefficient. The mass transfer coefficient has a significant effect on the performance of the porous electrode.

The mass transfer performance of an electrode is often characterized by the product of mass transfer coefficient and effective surface area of the electrode. The mass transfer property of various porous metal electrode materials has been studied during the past few decades. Marracino et al.[15] studied the mass transfer performance of a porous nickel with a high porosity (0.95–0.96) and found that the mass transfer performance of the porous nickel electrodes is about 10 times higher than that of the micromesh expanded nickel electrodes. Langlois and Coeuret[16] and Connect et al.[17] studied the SORAREC porous nickel which is manufactured by a metal decomposition method.[18] They reported that the mass transfer coefficient of this type of porous nickel decreases with pore size. Zhou et al.[19] investigated porous copper fiber sintered felt (PCFSF) with three different porosities (0.7, 0.8, and 0.9) and found that a porosity of 0.8 gave the best mass transfer property.

The good mass transport performance of porous metals is mainly derived from their high surface areas. Recio et al.[20] demonstrated that a nickel electrode made by electrodepositing nanostructured Ni on a stainless steel plate had mass transfer performance nearly 23 times that of a mirror polished nickel electrode, due to increased effective surface area. The mass transfer performance of electrodes is also affected by fluid conditions. Using turbulence promoters (TP) can increase the mass transfer coefficient by 1.7–3.8 times.[20–22] Increasing the electrolyte flow velocity can improve the mass transfer performance, but it is not always feasible due to high flow resistance and pumping power constraints.[23]

Porous structures vary dramatically with manufacturing processes.[9,24–26] Although several types of porous metals have been demonstrated to have attractive electrochemical properties, no research has been published to date on the mass transfer properties of porous metals manufactured by the space holder methods. This type of porous metals has unique porous structures with high specific surface areas and is expected to have superior mass transfer performance as electrode materials.[27]

This paper investigates the mass transfer coefficient of porous nickel manufactured by t12he Lost Carbonate Sintering (LCS) process at different electrolyte flow velocities. The LCS process is a representative space holder method for manufacturing porous

P. Zhu, Prof. Y. Zhao
School of Engineering, University of Liverpool,
Liverpool L69 3GH, UK
E-mail: sgpzhu@liverpool.ac.uk
The ORCID identification number(s) for the author(s) of this article can be found under https://doi.org/10.1002/adem.201700392.

DOI: 10.1002/adem.201700392

metals.[28,29] The LCS porous nickel has a highly controllable open-cell structure with a wide range of porosity and pore size. This work studies the effects of porosity and pore size on mass transfer coefficient and compares the mass transfer performance of the LCS nickel with other porous nickel electrodes reported in the literature.

2. Experimental Methods

Preparation of Nickel Electrodes: A solid nickel plate with a thickness of 1 mm and surface area of 2.8 cm^2 was used as a comparator. It was first ground by silicon carbide papers (grades 120, 600, and 1200) to achieve a finish about 15 μm, then polished by oil-lubricated diamond compounds on a woven cloth substrate to achieve a finish of 1 μm, and finally polished by 0.04 μm silk-type cloth pad before use.

Eighteen porous nickel samples, with porosity ranging from 0.55 to 0.75 and pore size ranging from 250 to 1500 μm, were manufactured by the LCS process.[28,29] The samples were cut by an electrical discharge machine (Prima E250, ONA Ltd., Bristol, UK) into a cylindrical shape with a diameter of 6 mm and a length of 5 mm. **Figure 1** shows a typical microstructure of the LCS porous nickel.

Before electrochemical tests, the porous nickel and nickel plate samples were first washed by 10% HCL solution to remove oxides on the surface and then rinsed in distilled water. The porous samples were placed in an agitated sacrificial electrolyte solution before being transferred to the electrochemical cell, in order to improve the infiltration of electrolyte in the pores.

Surface Areas Measurement: The geometric surface area of the LCS porous nickel samples was measured by the quantitative stereology method. The real surface area was measured by the double layer capacitance method. The detailed information of the measurement methods can be seen in published work.[1] For real surface area measurement, it should be noticed that the double layer capacitance of the LCS porous nickel was equal to half of the difference rather than the difference between the charge and discharge current over the applied scan rate. A typical plot for the LCS porous nickel sample in real surface area measurement at a scan rate range of 0.05–0.5 V s^{-1} can be seen in **Figure 2**. The counter electrode was Pt coil and the reference electrode was Saturated Calomel Electrode (SCE). The electrolyte was 8 M KOH. The specific capacitance of nickel in 8 M KOH is about 28 μF cm^{-2}.[30]

Mass Transfer Measurement: Experimental Apparatus: **Figure 3**a is a schematic diagram of the mass transfer experimental apparatus. It consists of a plastic electrolyte reservoir, a peristaltic pump (Masterlex L/S Computer-Compatible Digital Pump), a three electrode cell, a potentiostat (Autolab PGSTAT101), and a computer. The sample to be tested served as the working electrode. A water proof shrinkage tube was used to connect the porous nickel sample to an acrylic tube with an outer diameter of 6 mm (Figure 3b). The nickel plate was inserted into the acrylic tube, parallel to the tube and the flow of the electrolyte (Figure 3c). The electrolyte was forced to pass through the porous electrode, or flow past the solid plate electrode, and exhausted by the peristaltic pump.

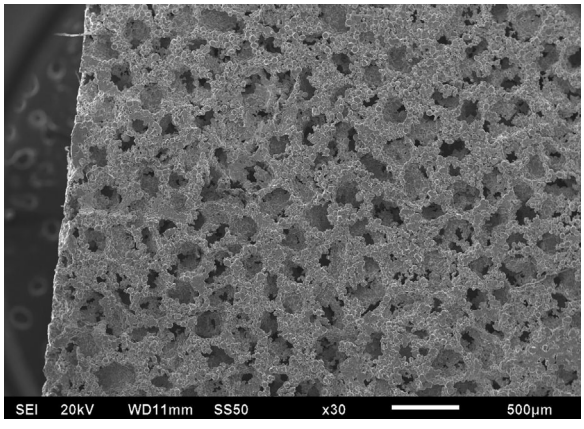

Figure 1. SEM image of the porous nickel manufactured by the lost sintering carbonate process.

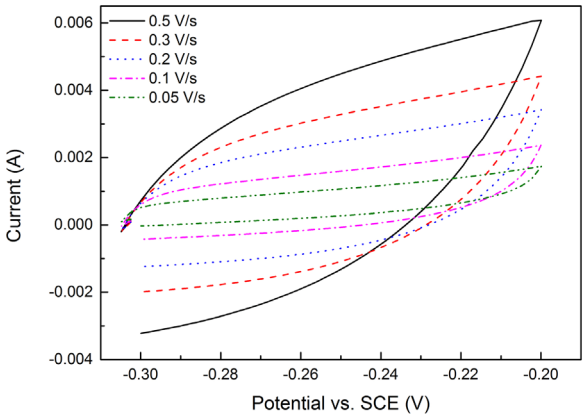

Figure 2. Typical current vs potential plot for LCS porous nickel sample in real surface area measurement at a scan rate range of 0.05–0.5 V s^{-1}.

Limiting Current Technique: The limiting current technique was used to measure the mass transfer coefficient. The electrochemical reaction used in this work was the reduction of the ferricyanide ion:

$$\left[Fe(CN)_6\right]^{3-} + e^- \rightarrow \left[Fe(CN)_6\right]^{4-} \quad (1)$$

A 1 M Na_2CO_3 was used as the background electrolyte. In characterizing the nickel plate electrode, the electrolyte contained 10^{-3} M $K_3Fe(CN)_6$ and 10^{-2} M $K_4Fe(CN)_6$. In characterizing the LCS porous nickel electrodes, the concentrations of the reactive species were reduced by 10 times and the electrolyte contained 10^{-4} M $K_3Fe(CN)_6$ and 10^{-3} M $K_4Fe(CN)_6$. This is because porous metals have high surface areas,[1] which can generate high currents, causing distortions in the measurements due to uncompensated solution resistance. Reducing the concentrations of the reactive species eliminated the effect of uncompensated solution resistance.[31] The limiting current was measured by linear sweep voltammetry at a scan rate of 5 mV s^{-1}, with an applied potential in the range from 0.2 V to −1.2 V.

Determination of Mass Transfer Coefficient: **Figure 4** shows a typical current-potential plot of a LCS porous nickel electrode. There are three regions in the curve, that is, hydrogen evolution, mass transfer control, and mixed control regions, which signify different transfer mechanisms. The limiting current, I_L, was determined from the mass transfer region and the mass transfer coefficient, k, was calculated by:

$$k = \frac{I_L}{nFAC} \quad (2)$$

where n is the number of electrons exchanged in the reaction ($n = 1$ for Eq. 2), F is the Faraday constant, A is the real surface area of the working electrode, and C is the bulk concentration of the electroactive species. The error of the mass transfer coefficient value mainly resulted from the error of the experimental measurement of limiting current, which was about 5%.

3. Results and Discussion

3.1. Effects of Porosity and Pore Size

Table 1 shows the structural properties of the LCS porous nickel samples, including nominal porosity, volumetric geometric

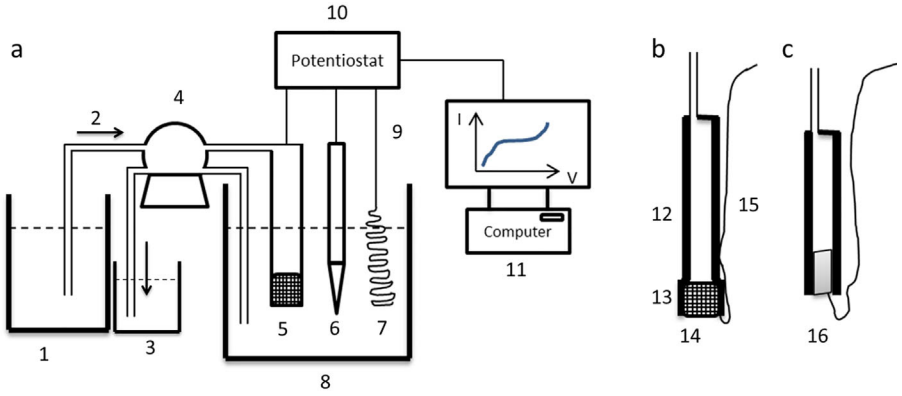

Figure 3. Schematics of a) mass transfer experimental apparatus, b) porous nickel working electrode, and c) nickel plate working electrode: 1) electrolyte reservoir, 2) pumping pipe, 3) waste solution reservoir, 4) peristaltic pump, 5) working electrode, 6) reference electrode (SCE), 7) counter electrode (platinum coil), 8) glass beaker, 9) wire, 10) potentiostat, 11) computer, 12) acrylic tube, 13) water proof shrinkage tube, 14) LCS porous nickel sample, 15) nickel wire, and 16) solid nickel plate.

surface area, and volumetric real surface area. The actual porosity of a sample is slightly different from the nominal porosity, depending on the manufacturing conditions. Volumetric surface areas designate surface areas per unit volume of sample. The geometric surface area is the surface area of the primary pores formed by the decomposition of the space holder particles, assuming a smooth surface. The real surface area takes into account all the surface area that can be reached by the electrolyte and contribute to the electrochemical reactions.

Figure 5 shows the variations of the mass transfer coefficient with sample porosity at different electrolyte flow rates in the range of 0.28–1.87 mL s^{-1} for LCS porous nickel samples with various pore size ranges. For the conditions investigated in this work, the mass transfer coefficient of the LCS porous nickel is in the range of 0.00069–0.0135 cm s^{-1}. For any given electrolyte flow rate, the mass transfer coefficient decreases with porosity, more pronounced at high electrolyte flow rates than at low flow rates. Comparing Figure 5ad shows that the mass transfer coefficient increases with pore size for the samples with a fixed porosity and electrolyte flow rate. The reason behind the effects of porosity and pore size will be discussed in Section 3.3.

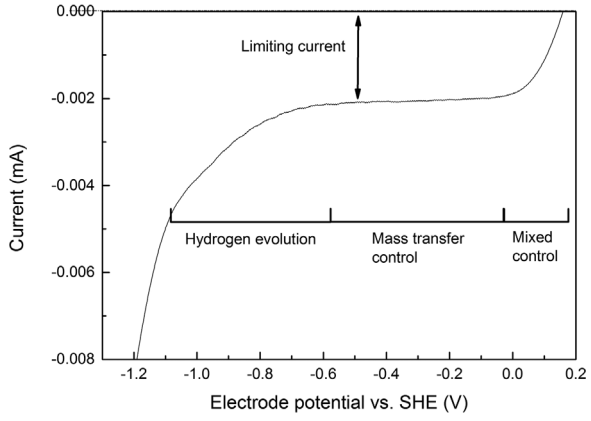

Figure 4. Typical current versus potential plot for the reduction of $Fe(CN)_6^{-3}$ in 10^{-4} M $K_3Fe(CN)_6 + 10^{-3}$ M $K_4Fe(CN)_6 + 1$ M Na_2CO_3 at a porous nickel electrode with a scan rate of 0.005 V s^{-1}.

3.2. Effect of Flow Velocity

It is shown in Figure 5 that the mass transfer coefficient of the LCS porous nickel samples increases with the electrolyte flow rate. While it is convenient to describe the mass transfer performance of a porous sample at an overall electrolyte flow rate, the effect of flow rate is better understood by the resultant flow velocity in the pore channels. The internal flow velocity, u, can be determined by:

$$u = \frac{Q}{A_C \varepsilon} \tag{3}$$

where Q is the flow rate of the electrolyte, A_C (0.283 cm^2) is the cross-sectional area of the flow channel, that is, the acrylic tube, and ε is the porosity of the porous nickel sample.

Figure 6 shows the variations of the mass transfer coefficient of the porous nickel samples with internal flow velocity, plotted in the logarithmic scale. The data for the solid nickel plate are also presented for comparison. The mass transfer coefficient increases exponentially with electrolyte flow velocity, which agrees well with the literature.[17,20] The relation between mass transfer coefficient, k, and internal flow velocity, u, can be described by[16,17]:

$$k = au^b \tag{4}$$

where a is a constant associated to the structural properties of the working electrode and b is a constant dependent on the

Table 1. Structural properties of the LCS porous nickel samples.

Porosity	Volumetric geometric surface area (cm^{-1})					Volumetric real surface area (cm^{-1})				
Pore size (μm)	0.55	0.60	0.65	0.70	0.75	0.55	0.60	0.65	0.70	0.75
250–425	68	76	82	90	96	948	789	637	593	457
425–710	42	50	54	56	60	687	632	529	461	342
710–1000	28	–	34	36	42	591	–	619	560	417
1000–1500	20	–	26	30	34	639	–	570	551	325

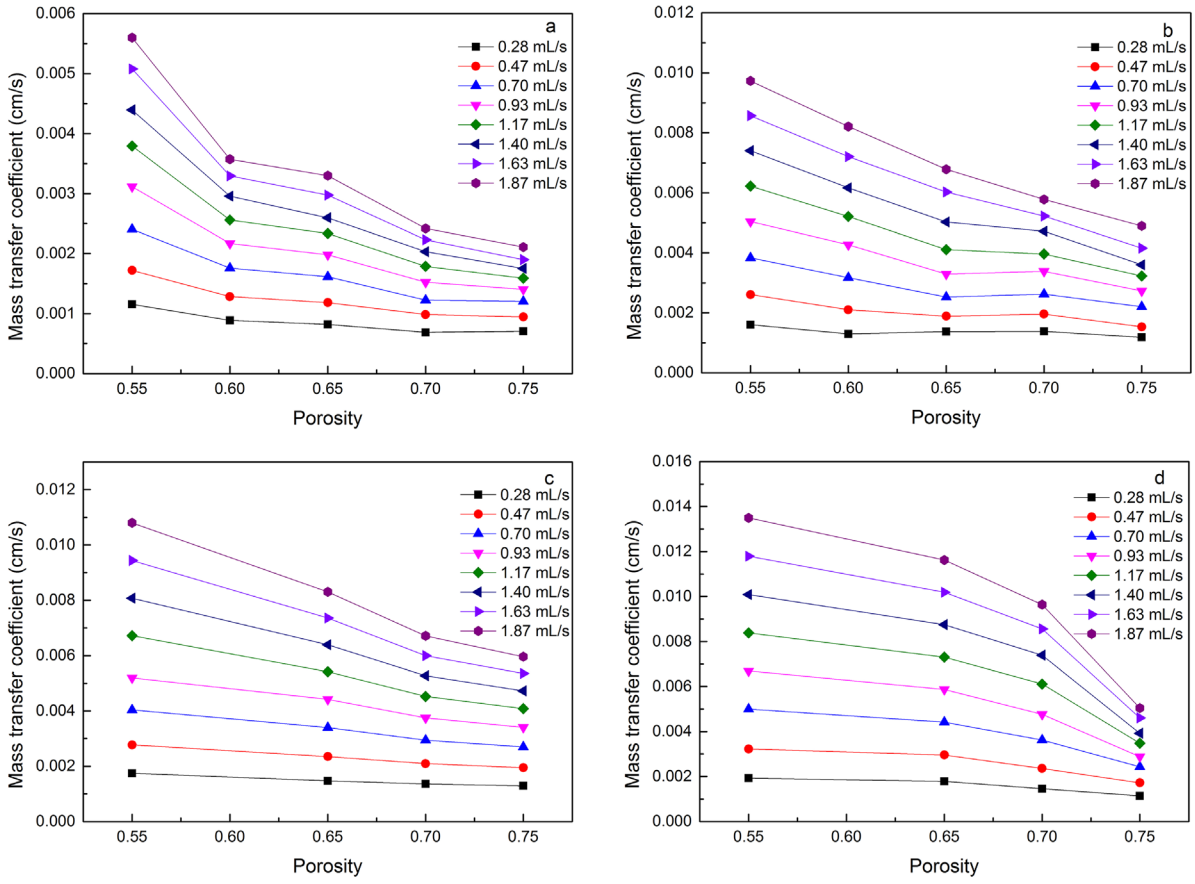

Figure 5. Mass transfer coefficient as a function of porosity at different electrolyte flow rates for the LCS porous nickel samples with various pore sizes: a) 250–425 μm, b) 425–710 μm, c) 710–1000 μm, and d) 1000–1500 μm.

hydrodynamic regime. The value of the exponent *b* can serve as an indicator of the nature of the flow.[20] The value of *b* is higher in a turbulent flow than in a laminar flow.[32]

3.3. Interpretation of the Effects of Porosity and Pore Size

Figure 7 shows the variations of the pre-exponential constant, *a*, and the exponent, *b*, in Equation 4 as a function of geometric surface area for the LCS porous nickel samples. The values of *a* and *b* were obtained from Figure 6 and the values of the geometric surface area are shown in Table 1. It is shown that the pre-exponential constant *a* and the exponent *b* are strongly correlated with the geometric surface area. The higher the volumetric geometric surface area, the lower the pre-exponential constant *a* and the exponent *b*.

The effect of geometric surface area on the constant *a* may arise from its effect on the spatial distribution of the electrolyte in the porous channels. For a fixed porosity, different geometric surface areas lead to different depths of electrolyte in the porous channel. A higher volumetric geometric surface area means a thinner electrolyte near the surface of the metal matrix, that is, the electrolyte being spread more thinly against the surface. If the depth of the electrolyte becomes comparable to or even thinner than the Nernst diffusion layer,[1,33] it can cause exhaustion of the reactive species. This may effectively lead to a reduced bulk concentration of the reactive species, which in turn can result in a reduced pre-exponential constant.

Geometric surface area is probably not a direct causative parameter for the exponent *b*. The exponent is an indicator of flow turbulence,[20] which is more likely affected by the tortuosity of the porous structure. Tortuosity of a porous medium characterizes the convoluted pathways, or channels, formed by pores through the porous medium. It is defined as the ratio of the average length of pathways between two points to the straight-line distance between the points in the porous medium. Lower porosities and large pores in LCS porous metals generally result in high tortuosity values.[34] At the same time, Lower porosities and large pores lead to lower volumetric geometric surface area. A low volumetric geometric surface area is therefore associated with a high tortuosity and high turbulence, resulting in a high exponent value.

Figure 7 also shows that the effects of porosity and pore size on the constants are different, although both affect the volumetric geometric surface area. The pre-exponential constant *a* increases significantly with pore size but does not change much with porosity for any given pore size. The effect of pore size can be explained by the relative magnitudes of the electrolyte reservoir and the diffusion layer. On the one hand, smaller pores

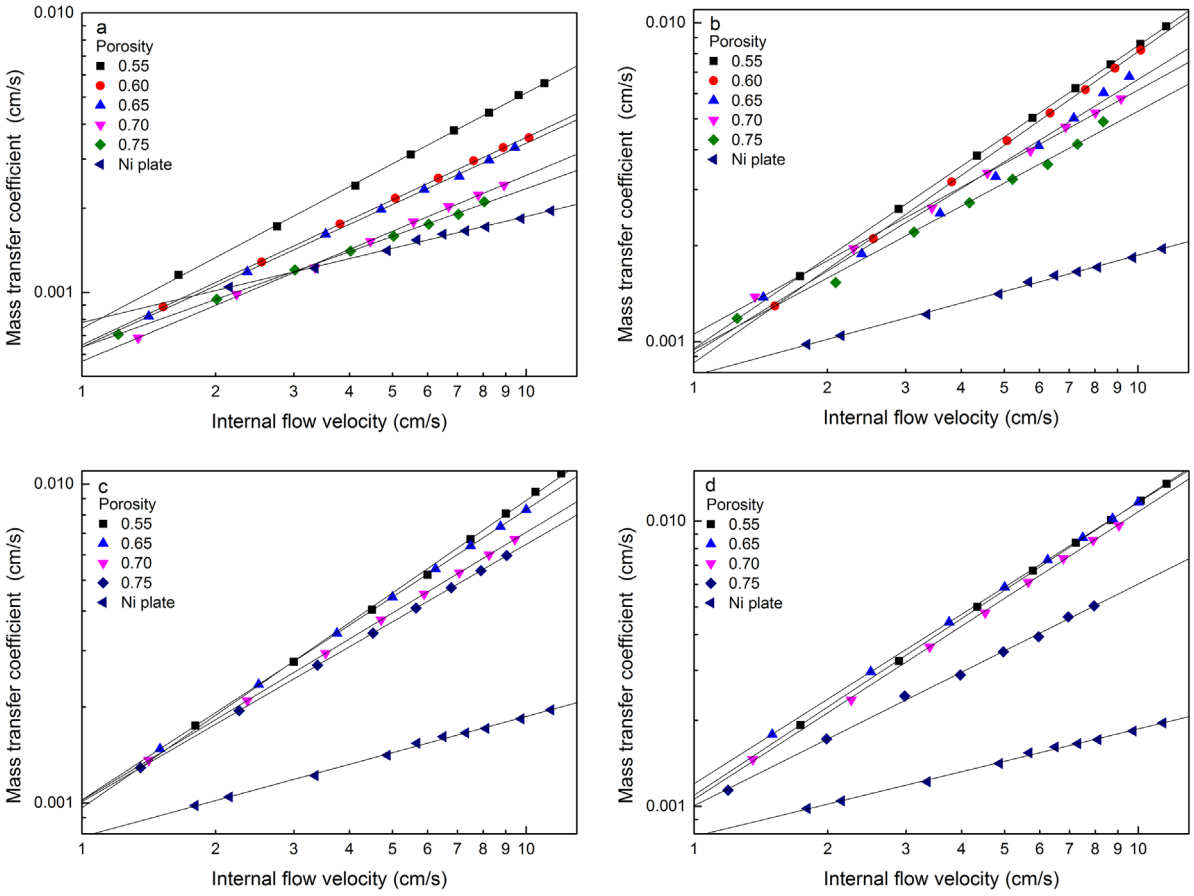

Figure 6. Mass transfer coefficient as a function of electrolyte flow velocity for the LCS porous nickel samples with pore sizes of: a) 250–425 μm, b) 425–710 μm, c) 710–1000 μm, and d) 1000–1500 μm.

contain smaller pockets of electrolyte and thus thinner electrolyte. On the other hand, smaller pores have greater surface curvatures and consequently thicker diffusion layers. The higher ratios between diffusion layer and electrolyte depth can lead to more severe exhaustion of reactive species and thus a reduced pre-exponential constant. The exponent *b* generally decreases significantly with porosity, but does not change as much with pore size for any given porosity. Although the porous nickel samples with the smallest pore size (250–425 μm) show lower exponent values, the samples with the other pore sizes have similar exponent values. These results indicate that the spatial distribution of the electrolyte is mainly influenced by pore size while the flow turbulence is mainly dependent on porosity.

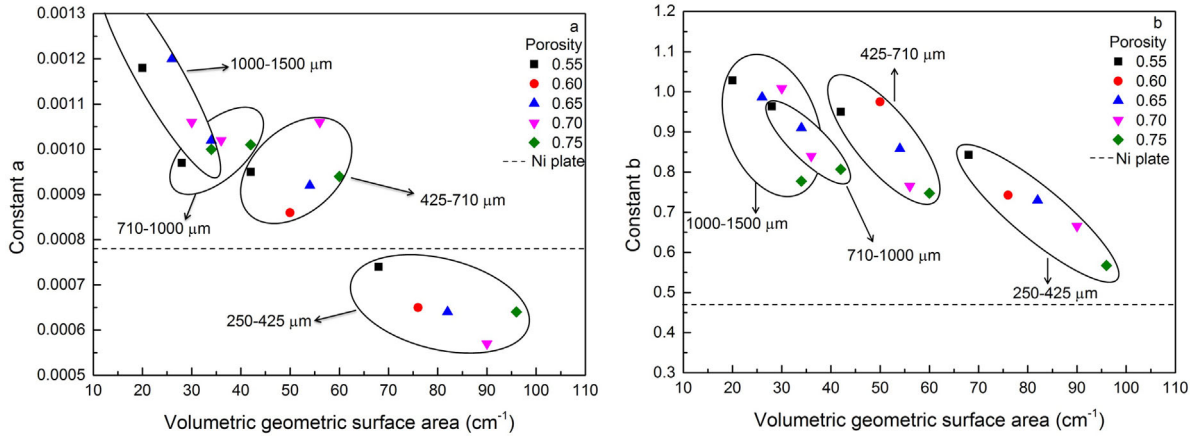

Figure 7. Variations of a) pre-exponential constant a and b) exponent b with volumetric geometric surface area.

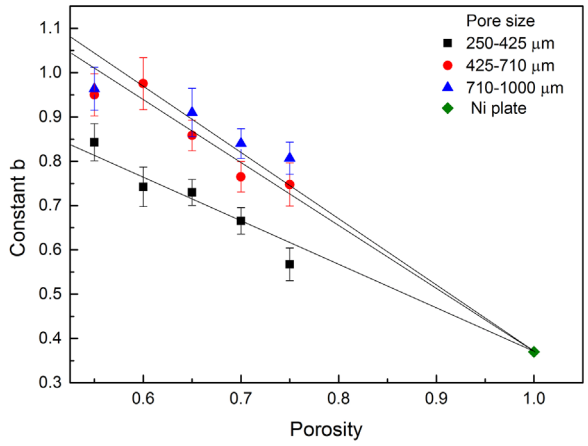

Figure 8. Variation of exponent b with porosity at different pore sizes.

3.4. Comparison with the Solid Nickel Electrode

Figure 6 shows that nearly all the LCS porous nickel samples have higher mass transfer coefficients (up to seven times) than the solid nickel plate at the same electrolyte flow velocities. This is very likely because the LCS porous structure promotes a highly turbulent flow, which is well known to lead to a high mass transfer coefficient.[32] The exception is the samples with the smallest pores of 250–425 μm at low electrolyte velocities, which have mass transfer coefficients similar to those of the nickel plate at the same velocity (Figure 6a). This is because the flow within the LCS porous nickel samples with small pores may remain laminar at low flow velocities, as in the case of the flow on the surface of a nickel plate.

The mass transfer performance of porous electrodes depends not only on the mass transfer coefficient but also on the internal surface area. The mass transfer performance is described by the product of the mass transfer coefficient and the real surface area (kA). The volumes of the porous nickel samples and nickel plate used in this study are almost identical, about 0.14 cm^3. The porous nickel samples have a geometric surface area in the range of 2.83–13.56 cm^2 and a real surface area in the range of 45–135 cm^2, which are about 1–5 times and 16–50 times of the surface area of the solid nickel plate (2.8 cm^2). Given that the porous nickel samples have a mass transfer coefficient 1–7 times of that of the solid nickel plate at the same electrolyte flow velocities, the mass transfer performance (kA) of the LCS porous nickel can be up to 300 times better than the solid nickel plate.

The limiting current can also be used as a direct indicator of the mass transfer performance, provided the electrodes to be compared are measured under the same conditions with the same electrolyte concentrations. The maximum limiting current of the porous nickel samples was 0.0131 A, which is about 30 times of the limiting current of the nickel plate measured at the same electrolyte velocity (0.0046 A). However, the concentration of Ferricyanide used in the measurements for the nickel plate was 10 times higher than that used in the measurements for the porous nickel samples. The mass transfer performance of the porous nickel is therefore up to 300 times better than the solid nickel plate, the same conclusion as reached by comparing kA.

The value of pre-exponential constant a for the solid nickel working electrode is 0.00078, which is higher than the a values of the LCS porous nickel samples with the smallest pore size (250–425 μm) but lower than those of the porous samples with larger pore sizes (Figure 7a). The value of exponent b for the solid nickel working electrode is 0.37, which is similar to the value reported in the literature for a fully developed laminar flow (≈0.33).[32] This indicates that, in the range of flow velocity studied in this work (1–12 cm s^{-1}), the electrolyte flow on the surface of the nickel plate remains laminar. The values of b for the porous nickel electrodes, however, are much higher, ranging from 0.57 to 1.03 (Figure 7b). The flow within the LCS porous structure can change to turbulence flow, due to the highly tortuous nature of the pore channels.

Figure 8 replots the constant b values against the porosity values of the LCS porous nickel samples. It is interesting to note that the trend lines for the samples with pore sizes of 250–425 μm, 425–710 μm, and 710–1000 μm approach 0.37 at a porosity of 1, that is, the b value of the nickel plate, which can be seen as a "porous sample" with a porosity of 1. The data points for the samples with a

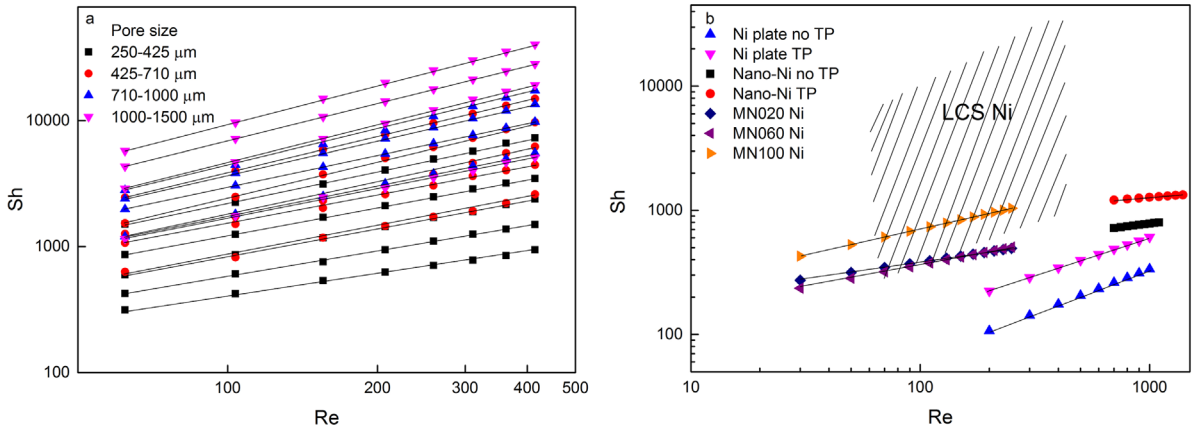

Figure 9. Correlation between Sherwood and Reynolds numbers for a) LCS porous nickel samples and b) various nickel electrodes. For each pore size range in a), the lines correspond to porosities of 0.55, 0.60, 0.70, and 0.75 (from top to bottom). The legends in b) designate solid Ni plate in the absence and presence of a TB,[23] nanostructured Ni in the absence and presence of a TB,[20] Ni foam MN020, MN060, and MN100.[17]

Table 2. Constants α and β for the porous nickel samples.

Pore size (μm)	α					β				
Porosity→	0.55	0.60	0.65	0.70	0.75	0.55	0.60	0.65	0.70	0.75
250–425	45.53	40.2	29.28	27.2	30.35	0.84	0.74	0.73	0.67	0.57
425–710	48.69	27.31	33.22	44.1	27.17	0.95	0.98	0.86	0.77	0.75
710–1000	51.24	–	56.18	61.94	42.94	0.96	–	0.91	0.84	0.81
1000–1500	82.63	–	73.85	44.38	47.17	1.03	–	0.99	1.01	0.78

pore size of 1000–1500 μm do not show a clear trend, because the pore size is about one sixth of the diameter of the sample and the random arrangement of pores can result in significant experimental variability.

Figure 8 shows that the constant b decreases with porosity but increases with pore size. As a general trend, the enhancement of the mass transfer coefficient therefore decreases with porosity but increases with pore size (Figure 5). As discussed previously in Section 3.3, this is because tortuosity of the porous samples generally increases with decreasing porosity and increasing pore size and a high tortuosity in turn increases flow turbulence.[34]

3.5. Comparison with Other Nickel Electrodes

Mass transfer to a porous electrode can be characterized by three-dimensionless parameters, namely the Sherwood (Sh), Reynolds (Re), and Schmidt (Sc) numbers:

$$Sh = \frac{kd_e}{D} \tag{5}$$

$$Re = \frac{vd_e}{\upsilon} \tag{6}$$

$$Sc = \frac{\upsilon}{D} \tag{7}$$

where k is the mass transfer coefficient, d_e is the diameter of the flow channel, D is the diffusion coefficient of electroactive species, υ is the kinematic viscosity of the electrolyte, and v is the superficial or Darcian flow velocity of the electrolyte, which is simply the flow rate divided by the cross-sectional area of the sample or the flow channel. In this work, the diameter of the flow channel $d_e = 0.6$ cm, the diffusion coefficient of ferricyanide ion $D = 6.4 \times 10^{-6}\,\mathrm{cm^2\,s^{-1}}$ and the kinematic viscosity of the electrolyte $\upsilon = 9.56 \times 10^{-3}\,\mathrm{cm^2\,s^{-1}}$.[20] It should be noted that in calculating the Sherwood number (Eq. 5) for the LCS porous nickel sample, the geometric surface area was used for calculating the mass transfer coefficient, k, instead of the real surface area as in Equation 2. This is to facilitate comparison with other electrode materials, because geometric surface area was often used to characterize the mass transfer performance of different types of electrodes in the literature.

Figure 9a shows the correlations between Sherwood and Reynolds numbers for the LCS porous nickel samples. The Sherwood number increases exponentially with the Reynolds number in the range of 60–415. The sample with a low porosity of 0.55 and a large pore size of 1000–1500 μm shows the highest Sherwood number (5770–40429), while the sample with a high porosity of 0.75 and a small pore size of 250–425 μm shows the lowest Sherwood number (315–942). Figure 9b compares the LCS porous nickel electrode with a number of other nickel electrodes and shows that the LCS porous nickel has superior performance in terms of the Sherwood number in a modest range of Reynolds number.

The relationship among the dimensionless parameters at a constant temperature can be expressed as[21–23,35,36]:

$$Sh = \alpha Re^{\beta} Sc^{0.33} \tag{8}$$

where α is a constant associated to the geometry and structure of the electrode and β is a constant dependent on the hydrodynamic regime. Constant β is the same as the constant b in Equation 4. Constant α is different from but related to the pre-exponential constant a in Equation 4.

Table 2 shows the values of α and β for the LCS porous nickel samples, obtained by fitting the experimental data to Equation 8. Constant α generally increases with pore size except for two samples. The two exceptions are likely due to the experimental errors or variability. The effect of porosity on constant α shows no clear trend. Constant β increases with pore size but decreases with porosity.

Table 3 shows the values of α and β for the LCS porous nickel samples in comparison with various nickel electrodes taken from the literature. The values of constant α of the LCS porous nickel samples are about 100–350 times higher than that of the nickel plate[23] and about 3–8 times higher than those of the nickel foams with a high porosity of 0.97.[17] This is because

Table 3. Constants α and β for various electrodes (TP stands for turbulence promoter).

Electrode		*Re*	α	β
LCS porous Ni	Porosity: 0.55–0.75 and Pore size: 1000–1500 μm	60–415	27.17–82.63	0.57–1.03
Ni plate[23,32]	No TP	200–1000	0.22	0.71
	With TP		0.74	0.62
	Laminar flow	<2300	2.54	0.33
	Turbulent flow	>2300	0.023	0.8
Ni foam[17]	MN020	30–250	10.8	0.28
	MN060		7.1	0.36
	MN100		10.5	0.42
Nano Ni[20]	Without a TP	250–1000	28.4	0.23
	With a TP		86.2	0.14

the LCS porous nickel has a large effective (real) surface area, which is about one to two orders of magnitude higher than its geometric surface area (see Table 1). For the nanostructured nickel electrode which was reported with a high effective surface area,[20] the values of constant α are comparable to that of the LCS porous nickel samples.

The values of constant β of the LCS porous nickel samples are similar to that of the nickel plate under turbulent flow but higher than that of the nickel plate under laminar flow.[32] They are considerably higher than those of the nickel foams[17] and the nanostructured nickel.[20]

4. Conclusions

1) The mass transfer coefficient of the LCS porous nickel samples with a porosity of 0.55–0.75 and a pore size of 250–1500 μm was measured at an electrolyte flow velocity range from 1 to 12 cm s^{-1}.
2) The mass transfer coefficient of the LCS porous nickel is in the range 0.0007–0.014 cm s^{-1}. It increases with pore size and decreases with porosity.
3) At low flow velocities, the mass transfer coefficient is similar to that of the nickel plate. At high flow velocities, it can be up to seven times larger than that of the nickel plate due to turbulence. The mass transfer performance (kA) of the LCS porous nickel samples is up to 300 times better than the nickel plate.
4) The LCS porous nickel has higher Sherwood numbers than many other nickel electrodes in the modest range of Reynolds number, due to its high real surface area and its tortuous porous structure, which promotes turbulent flow.

Conflict of Interests

The authors declare no conlfict of interest.

Keywords

porous nickel; mass transfer coefficient; lost carbonate sintering; Sherwood number surface area

Received: April 29, 2017
Revised: June 7, 2017
Published online: July 5, 2017

[1] K. K. Diao, Z. Xiao, Y. Y. Zhao, *Mater. Chem. Phys.* **2015**, *162*, 571.
[2] E. Hernández-Nava, C. Smith, F. Derguti, S. Tammas-Williams, F. Léonard, P. Withers, I. Todd, R. Goodall, *Acta Mater.* **2015**, *85*, 387.
[3] N. Hampson, J. Lee, K. Macdonald, *J. Electroanal. Chem. Interfacial Electrochem.* **1972**, *34*, 91.
[4] J.-F. Despois, A. Mortensen, *Acta Mater.* **2005**, *53*, 1381.
[5] Z. Xiao, Y. Zhao, *J. Mater. Res.* **2013**, *28*, 2545.
[6] A. Otaru, A. R. Kennedy, *Scripta Mater.* **2016**, *124*, 30.
[7] J.-F. Despois, R. Mueller, A. Mortensen, *Acta Mater.* **2006**, *54*, 4129.
[8] C. San Marchi, A. Mortensen, *Acta Mater.* **2001**, *49*, 3959.
[9] M. F. Ashby, T. Evans, N. A. Fleck, J. Hutchinson, H. Wadley, L. Gibson, *Metal Foams: A Design Guide*, Elsevier, Oxford, UK **2000**.
[10] V. Tracey, N. Williams, *Electrochem. Technol.* **1965**, *3*, 17.
[11] K. C. Liu, M. A. Anderson, *J. Electrochem. Soc.* **1996**, *143*, 124.
[12] R. Singh, H. Kasana, *Appl. Therm. Eng.* **2004**, *24*, 1841.
[13] F. P. Incropera, A. S. Lavine, T. L. Bergman, D. P. DeWitt, *Fundamentals of Heat and Mass Transfer*, Wiley, New York, US **2007**.
[14] A. J. Bard, L. R. Faulkner, J. Leddy, C. G. Zoski, *Electrochemical Methods: Fundamentals and Applications*, Wiley, New York, **1980**.
[15] J. Marracino, F. Coeuret, S. Langlois, *Electrochim. Acta* **1987**, *32*, 1303.
[16] S. Langlois, F. Coeuret, *J. Appl. Electrochem.* **1989**, *19*, 51.
[17] P. Cognet, J. Berlan, G. Lacoste, P.-L. Fabre, J.-M. Jud, *J. Appl. Electrochem.* **1995**, *25*, 1105.
[18] J. Babjak, V. A. Ettel, V. Paserin, Method of forming nickel foam, USA Patent US4957543 A **1990**.
[19] W. Zhou, Q. Wang, Q. Qiu, Y. Tang, J. Tu, K. Hui, K. Hui, *Fuel* **2015**, *145*, 136.
[20] F. Recio, P. Herrasti, L. Vazquez, C. P. de León, F. Walsh, *Electrochim. Acta* **2013**, *90*, 507.
[21] C. Brown, D. Pletcher, F. Walsh, J. Hammond, D. Robinson, *J. Appl. Electrochem.* **1992**, *22*, 613.
[22] M. Griffiths, C. P. de León, F. C. Walsh, *AIChE J.* **2005**, *51*, 682.
[23] C. Brown, D. Pletcher, F. Walsh, J. Hammond, D. Robinson, *J. Appl. Electrochem.* **1993**, *23*, 38.
[24] J. Park, S. Hyun, S. Suzuki, H. Nakajima, *Acta Mater.* **2007**, *55*, 5646.
[25] S. Deville, E. Saiz, A. P. Tomsia, *Acta Mater.* **2007**, *55*, 1965.
[26] D. T. Queheillalt, H. N. Wadley, *Acta Mater.* **2005**, *53*, 303.
[27] Y. Torres, J. Pavón, J. Rodríguez, *J. Mater. Process. Technol.*, **2012**, *212*, 1061.
[28] Y. Y. Zhao, T. Fung, L. P. Zhang, F. L. Zhang, *Scripta Mater.* **2005**, *52*, 295.
[29] Y. Y. Zhao, L. P. Zhang, *Proc. Inst. Mech. Eng. Part B: J. Eng. Manuf.* **2008**, *222*, 267.
[30] E. Gagnon, *J. Appl. Electrochem.* **1976**, *6*, 95.
[31] R. E. Smith, T. J. Davies, N. D. B. Baynes, R. J. Nichols, *J. Electroanal. Chem.* **2015**, *747*, 29.
[32] D. Szánto, P. Trinidad, I. Whyte, F. Walsh, Proc. of 4th European Symposium on Electrochemical Engineering: Contemporary Trends in Electrochemical Engineering, European Federation of Chemical Engineering, Prague, Czech Republic, **1996**.
[33] P. Zhu, Y. Zhao, *RSC Adv.* **2017**, *7*, 26392.
[34] K. K. Diao, L. P. Zhang, Y. Y. Zhao, *Measurement*, Measurement of tortuosity of porous Cu using a diffusion diaphragm cell, **2017** *110*, 335.
[35] W. Taama, R. Plimley, K. Scott, *Electrochim. Acta* **1996**, *41*, 543.
[36] K. Kinoshita, S. Leach, *J. Electrochem. Soc.* **1982**, *129*, 1993.